Catalysis Letters 53 (1998) 65–71

Surface acid property and its relation to SCR activity of phosphorus added to commercial $V_2O_5(WO_3)/TiO_2$ catalyst

Hiroyuki Kamata [a], Katsumi Takahashi [a] and C.U. Ingemar Odenbrand [b,*]

[a] *Research Institute, Ishikawajima-harima Heavy Industries Co., Ltd., 3-1-15 Toyosu, Koto-ku, Tokyo 135, Japan*
[b] *Department of Chemical Engineering II, Chemical Center, Lund University, Institute of Technology, PO Box 124, S-221 00 Lund, Sweden*

Received 14 January 1998; accepted 14 April 1998

To examine the influence of phosphorus on the commercial $V_2O_5(WO_3)/TiO_2$ SCR catalyst, measurements were carried out by means of infrared and Raman spectroscopy, XPS, and NO reduction measurement as a function of phosphorus loading. Phosphorus added to the catalyst was found to disperse well over the catalyst without a significant agglomeration up to 5 wt% P_2O_5 addition. The number of the hydroxyl groups bonded to the vanadium and titanium species decreased readily with increasing amount of phosphorus. Correspondingly, the hydroxyl groups bonded to the phosphorus species were formed. NH_3 adsorbed on both hydroxyl groups bonded to vanadium and phosphorus as ammonium ions, implying that the P–OH groups formed are also responsible for the Brønsted acidity. The NO reduction activity was found to be decreased with increasing amount of phosphorus; however, the influence of phosphorus was relatively small irrespective of the large amount of phosphorus addition. The deactivation might be caused by the change in the nature of the surface hydroxyl groups as Brønsted acid sites. Phosphorus species might partially wrap the surface V=O and W=O groups, which might also contribute to the deactivation.

Keywords: selective catalytic reduction, nitric oxide reduction, phosphorus, acid property

1. Introduction

The selective catalytic reduction (SCR) of nitric oxide (NO) by ammonia is one of the most successful technologies for NO_x emission control from stationary sources [1]. The most widely used catalyst for this purpose is the mixed oxides of V_2O_5 and WO_3, or MoO_3, supported on the anatase phase of a TiO_2 carrier. Although V_2O_5 is the active phase, its content is generally low, ~2 wt%, in the commercial catalysts. The surface vanadyl species disperse well in monomeric or polymeric forms over TiO_2 [2,3]. By comparison, WO_3, normally ~10 wt%, is also expected to provide thermal stability to the catalyst. The nature of an active phase, i.e., isolated and polymeric vanadium species, can be readily affected by small amounts of the additives, resulting in a possible deactivation when the flue gas contains trace amounts of metal compounds. So far, several studies have been made on the effect of the additives on the structures and the SCR activities for V_2O_5-supported TiO_2 catalysts [4–8]. The effect of alkaline or alkaline earth metal on the SCR activity has been studied for the V_2O_5/TiO_2 catalyst [4–6] and, also, for bulk V_2O_5 [7]. Chen and Yang [8] reported that alkaline metal oxides deactivated the V_2O_5/TiO_2 catalyst. The change in molecular structure of the surface species upon addition of compounds has been studied intensively by using Raman spectroscopy [9,10]. The surface structure of vanadium species is affected by the pH at the point of zero charge of the surface moisture layer, which, in turn, is dependent on the nature of additives, for example, acidic or basic compounds [9]. Under hydrated conditions, WO_3, Nb_2O_3, and SiO_2 are non-interacting; on the other hand, K_2O and P_2O_5 are interacting compounds from the point of view of the coordination between the additives and the surface vanadium species [10].

For the phosphorus compounds, it has been reported that the addition of phosphorus causes degradation of the SCR activity for the V_2O_5/TiO_2 catalyst [11]. The decrease in SCR activity was also observed for a $V_2O_5(WO_3)/TiO_2$ catalyst with the addition of H_3PO_4 as an extrusion binder [12]. Compared with the SCR catalyst, the phosphorus-doped V_2O_5/TiO_2 catalyst has been given much attention as an application in the oxidation of hydrocarbons [10,13–16]. Zhu et al. [14] reported that the phosphorus species added to the monolayer-type V_2O_5/TiO_2 catalyst decreased the activity of toluene oxidation and, also, changed the selectivity. A small effect of phosphorus was reported on the catalyst properties for up to 1.2 wt% P_2O_5 added to the V_2O_5/TiO_2 catalyst [15]. An enhancement of the acid properties by phosphorus was suggested for the V_2O_5/TiO_2 catalyst. The effect of phosphorus on the catalytic activity of hydrocarbon oxidation was found to depend on the type of the reaction process [16]. From studies on phosphorus added to the V_2O_5/TiO_2 catalyst, it was suggested that phosphorus compounds change the nature of the surface active sites for the catalytic oxidation of hydrocarbons. To understand the role of the surface species in the SCR reaction, it is worth examining how the phosphorus compounds change the nature of the active phase and their relation to the activity of the NO reduction.

* To whom correspondence should be addressed.

For the purpose mentioned above, we focused our attention on the effect of phosphorus addition on the acid properties of the $V_2O_5(WO_3)/TiO_2$ SCR catalyst. To obtain information on the industrial use, a commercial SCR catalyst, $V_2O_5(WO_3)/TiO_2$ with Si–Al–O fiber, was used. The change in the surface acid properties and the SCR activity on addition of the phosphorus oxide, P_2O_5, were examined by means of diffuse reflectance infrared spectroscopy (DRIFT) of NH_3 adsorption and SCR activity measurement. Raman spectroscopy and XPS analysis were also performed to examine the structure of the surface species.

2. Experimental

2.1. Catalyst

The catalyst used in this study was obtained by gently crushing and sieving a commercial honeycomb monolith into particles of 100–180 μm in diameter. The chemical composition of the catalyst was determined by a Perkin-Elmer Plasma 2000 ICP-AES; 1 wt% V_2O_5–8 wt% WO_3/TiO_2 (V : W : Ti = 0.012 : 0.028 : 0.96 in atomic ratio) with approximately 10 wt% silica–alumina fiber. Catalyst, added with phosphorus, was prepared by impregnation via incipient wetness with aqueous solutions of H_3PO_4. The impregnation was performed in small containers overnight to obtain a homogeneous distribution of phosphorus throughout the particles before drying at room temperature. Subsequently, the catalyst was dried at 383 K and then calcined at 723 K for 4 h under a stream of dry air.

2.2. Characterisation

The textural properties of the catalyst were determined by N_2 adsorption at 77 K (Micromeritics Co., ASAP 2400). Before the measurements, degassing was carried out at 423 K for 16 h.

DRIFT spectra were collected using a Mattson Polaris™ spectrometer with a Harrick Scientific Praying Mantis diffuse reflectance attachment. Adsorption measurements were carried out in a heatable reaction cell with a resolution of 4 cm^{-1}. The catalyst powder was preheated in the reaction cell at 593 K (3 h) under a stream of argon before adsorption was carried out. After being cooled to room temperature, the catalyst was exposed to a gas mixture of 1% NH_3 and Ar for 30 min before being purged by Ar for another 30 min. To examine the behaviour of NH_3 adsorbed on the catalyst upon heat treatment, the catalyst was heated from 373 to 573 K under a stream of argon in the IR cell and then cooled to room temperature for the collection of spectra. All spectra were collected at room temperature.

Raman spectra were recorded with a Bruker IFS66 FTIR spectrometer, equipped with an FRA 106 Raman device, with a resolution of 4 cm^{-1}. The laser power at the sample location was set to 50 mW. To examine the molecular structure upon dehydration, Raman spectra were also collected on increasing laser power from 50 to 200 mW.

XPS measurements were performed with a Kratos XSAM 800 instrument with standard Mg radiation. The analyser was operated at 80 eV of pass energy and at low magnification. The satellite was subtracted before the calculation of the intensities. Peak intensities were determined from the area above a linear base line.

2.3. Activity measurements

The NO reduction activity was measured at steady-state conditions in a plug-flow microreactor (5 mm in diameter) using an apparatus described in the literature [17]. The operating conditions were: total flow rate (STP) 900 ml/min; catalyst weight 0.08 g; total pressure $\approx$ 0.12 MPa; reaction temperature 533–673 K. The concentrations of reactants were 600 ppm NO, 700 ppm NH_3, and 2% O_2 (He balance). The concentrations of reactants and products were determined by mass spectrometry (Balzers, type QMG 311) using argon as an internal standard. The conversion of NO, X_{NO}, was calculated by the difference of the NO concentrations in the inlet and exit streams. The formation of nitrous oxide, N_2O, was sufficiently low (less than 8 ppm) up to 673 K for each catalyst tested.

3. Results and discussion

3.1. Influence of phosphorus on textural properties

The textural properties of the $V_2O_5(WO_3)/TiO_2$ catalyst with different P_2O_5 contents are summarised in table 1. With increasing P_2O_5 loading, both the specific surface area and the pore volume of the catalyst gradually decrease. In agreement with these changes, the average pore diameter increases with increasing amount of P_2O_5 loading. The change in the average pore diameter is mainly due to the decrease of the pores with radii less than 200 Å upon addition of phosphorus.

3.2. Dispersion of phosphorus species on the catalyst

Figure 1 shows the intensity ratios of $I_{P_{2s}}/I_{Ti_{2p}}$, $I_{P_{2s}}/I_{V_{2p}}$, and $I_{P_{2s}}/I_{W_{2p}}$ measured by XPS as a function of nominal P_2O_5 loading. All ratios increase almost linearly with increasing amount of P_2O_5 added to the catalyst. This indi-

Table 1
Textural properties of the $V_2O_5(WO_3)/TiO_2$ catalyst with different P_2O_5 contents.

	P_2O_5 loading (wt%)					
	0	0.5	1	2	3	5
Specific surface area (m^2/g)	64.3	63.0	61.0	57.9	55.4	52.4
Pore volume (cm^3/g)	0.280	0.279	0.272	0.264	0.257	0.240
Average pore diameter (Å)	174	177	179	183	186	184

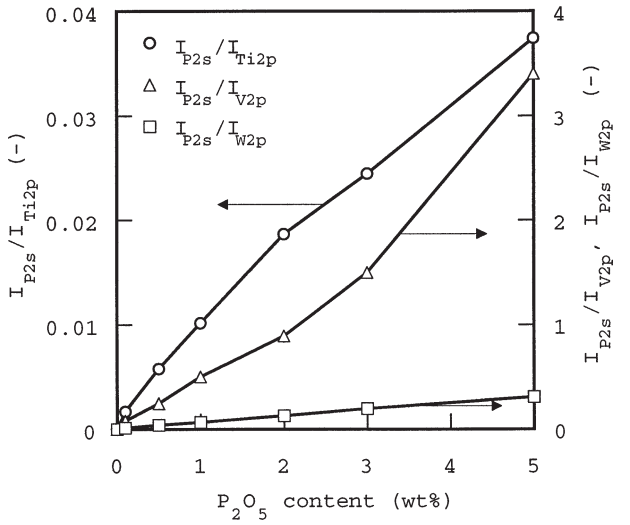

Figure 1. Intensity ratios of $I_{P_{2s}}/I_{Ti_{2p}}$, $I_{P_{2s}}/I_{V_{2p}}$, and $I_{P_{2s}}/I_{W_{2p}}$ as a function of nominal P_2O_5 content.

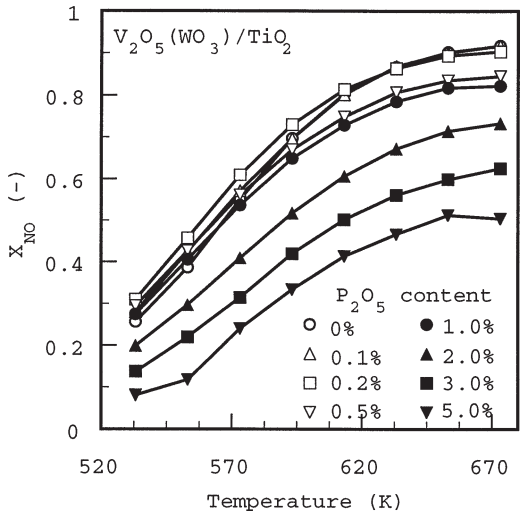

Figure 2. Temperature dependence of NO conversion, X_{NO}, for $V_2O_5(WO_3)/TiO_2$ catalyst with different amounts of P_2O_5. Experimental conditions were: total flow rate (STP) 900 ml/min (600 ppm NO, 700 ppm NH_3, 2% O_2, and He as balance), catalyst weight 0.08 g, and total pressure approximately 0.12 MPa.

cates that phosphorus disperses well over the catalyst surface without significant agglomeration. Since the intensity ratios of $I_{P_{2s}}/I_{V_{2p}}$ and $I_{P_{2s}}/I_{W_{2p}}$ increase in parallel with the increase of $I_{P_{2s}}/I_{Ti_{2p}}$, phosphorus might not preferentially coordinate to specific sites, such as vanadium species, during the preparation. On the surface of the catalyst without P_2O_5 addition, the existence of sulphur species was observed. According to the ICP result, the concentration of sulphur is approximately 94 μmol/g. The intensity of S_{2p} electron spectra was found to decrease nearly proportionally to the amount of P_2O_5, suggesting a decrease in the coverage of sulphur species on surfaces after phosphorus addition. There was no effect on the V_{2p}, W_{2p}, and Ti_{2p} electron spectra on addition of phosphorus.

3.3. NO reduction activity

Figure 2 shows the temperature dependence of the conversion of NO for the catalyst with different P_2O_5 loadings. For the catalyst without P_2O_5 addition, the conversion increases with temperature up to 0.92 at 673 K. For the catalyst in which lower amount of P_2O_5 was added, no pronounced effect upon addition of P_2O_5 on the activity is observed; however, the conversion decreases gradually with increasing amount of P_2O_5, particularly at higher temperatures. With increasing amount of P_2O_5 loading, the effect on the activity becomes more significant. However, even the catalyst with 5 wt% P_2O_5 still retains, to a certain extent, NO reduction activity, $X_{NO} \approx 0.5$ at 673 K. Compared with the effect of alkaline metal oxides, such as K_2O [18], phosphorus has little effect on the NO reduction activity of a commercial SCR catalyst. This behaviour is essentially consistent with the effect caused by the addition of P_2O_5 on NO reduction over V_2O_5/TiO_2 catalyst [11].

Well dispersed phosphorus can be expected to modify the surface species. Thus, the observed deactivation is not only caused by the change in the textural property, but also by the alteration of the active sites on the surface.

3.4. Change in the nature of the surface acid sites on the catalysts

3.4.1. Surface acid sites on the $V_2O_5(WO_3)/TiO_2$ catalyst

Figure 3 shows typical DRIFT spectra of NH_3 adsorption on the catalyst without P_2O_5 addition. After being heated at 593 K for 3 h under a streeam of argon, the bands at 3672 and 3742 cm^{-1}, which are due to surface hydroxyl groups bonded to titanium, ν_{Ti}(OH) [19,20], are observed (spectrum (A) of figure 3(b)). The band due to V–OH groups, ν_V(OH), is also confirmed at 3640 cm^{-1} [20]. The band due to hydroxyl groups bonded to the surface wolfram atoms is not clearly distinguished. Further information on the surface OH groups on WO_3 is still needed. As expected from the XPS result, a weak band, which may correspond to surface sulphate species, was observed at 1378 cm^{-1} (spectrum (A) of figure 3(a)). The sulphur species might enhance the strength of the acidity of the catalyst surface [19].

After the catalyst is exposed to gaseous ammonia, as expected, the bands due to the NH_3 species adsorbed on the surface are observed at 1432, 1666, and 1609 cm^{-1}. They have been assigned to $\delta_{as}(NH_4^+)$, $\delta_s(NH_4^+)$, and $\delta_s(NH_3)$, respectively (spectrum (B) of figure 3(a)) [21,22]. The Brønsted and Lewis acid sites correspond to the adsorption sites for ammonium ions, NH_4^+, and coordinatively adsorbed NH_3, respectively. As to the surface hydroxyl groups, the intensity of the ν_V(OH) band readily decreases after being exposed to gaseous NH_3. Compared with the change in the intensity of the ν_V(OH) band, the ν_{Ti}(OH) band (at 3672 cm^{-1}) is not significantly affected by the NH_3 adsorption (spectrum (B) of figure 3(b)). This suggests that the V–OH groups are responsible for the sites, where NH_3 adsorbs as ammonium ions, i.e., NH_3 preferentially adsorbs on the V–OH groups. The band due to

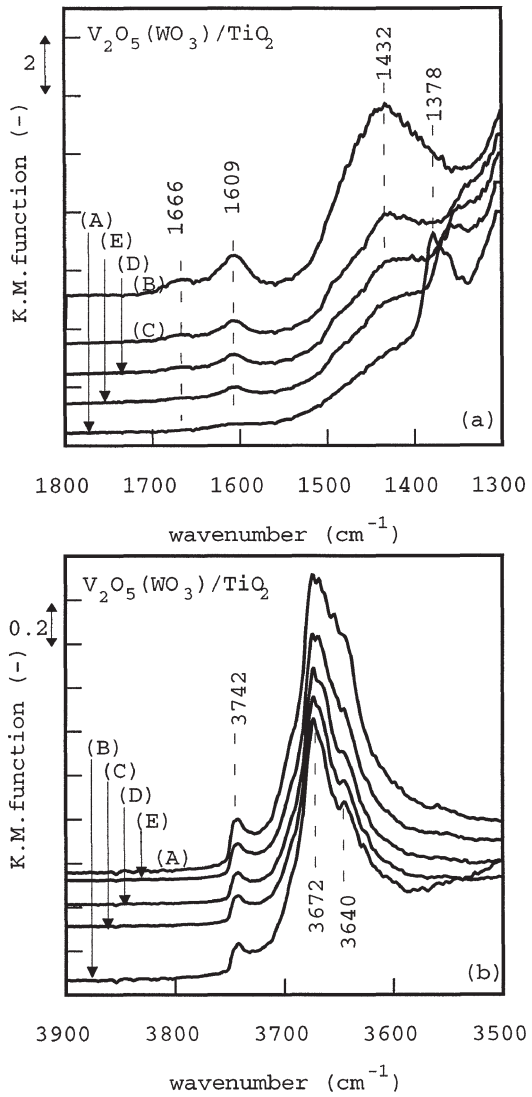

Figure 3. DRIFT spectra of NH_3 adsorption on $V_2O_5(WO_3)/TiO_2$ without P_2O_5 addition. Two spectral regions, 1800–1300 and 3900–3500 cm^{-1}, are shown in (a) and (b), respectively. (A) After being heated at 593 K under flowing argon for 3 h, (B) after being exposed to gaseous NH_3 for 30 min and subsequently purged by argon for 30 min at room temperature, and (C)–(E) after being heated at 473 (C), 523 (D), and 573 K (E) under a stream of argon. All spectra were collected at room temperature.

the surface sulphate species disappears, when the catalyst is exposed to gaseous NH_3.

After subsequent heating at higher temperatures under a stream of argon, the bands due to the ammonium ions and coordinatively adsorbed NH_3 decrease in intensity, as shown in figure 3(a). From the comparison of the change in intensity of these bands, the adsorbed NH_3 on the Lewis acid sites is more stable against temperature than ammonium ions. The reduced intensity of the ν_V(OH) bands upon NH_3 adsorption is restored toward its original shape according to the desorption of NH_3. The band due to the surface sulphate species is restored at a somewhat lower wavenumber after the heat treatment (473 K) (compare spectra (A) and (C) of figure 3(a)). The band due to sulphate species increases in intensity slowly with increasing activation temperature. The band position also shifts toward its original position. This suggests that chemisorbed NH_3 also interacts with the surface sulphate species.

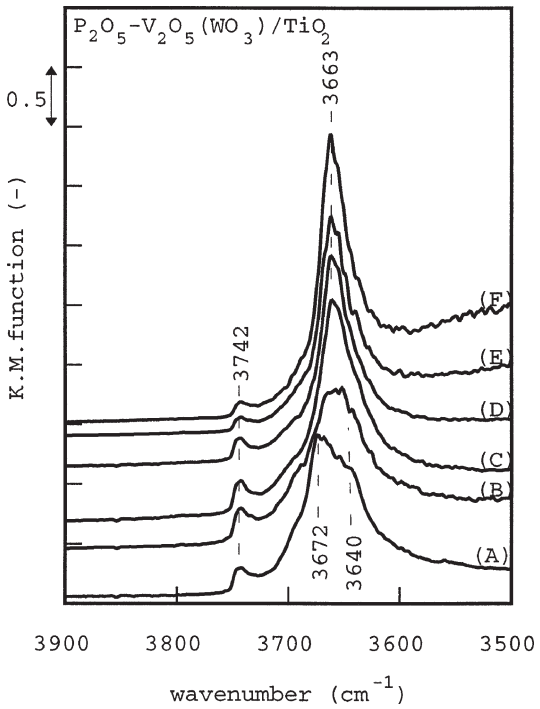

Figure 4. DRIFT spectra in the OH region of $V_2O_5(WO_3)/TiO_2$ with different P_2O_5 contents after being heated at 593 K under a stream of argon for 3 h. (A) 0, (B) 0.1, (C) 1, (D) 2, (E) 3, and (F) 5 wt% P_2O_5.

3.4.2. Change in the nature of acid sites on the $V_2O_5(WO_3)/TiO_2$ catalyst with P_2O_5 addition

Figure 4 shows the DRIFT spectra in the OH region for the catalyst with different P_2O_5 contents after being heated at 593 K under a stream of argon. The ν_{Ti}(OH) and ν_V(OH) bands (at 3672 and 3640 cm^{-1}, respectively, in spectrum (A) of figure 4) readily decrease in intensity with increasing amount of phosphorus. For the sample with P_2O_5 addition, the band due to the hydroxyl group bonded to phosphorus, ν_P(OH), is found at 3663 cm^{-1} [14]. In accordance with the decrease in intensity of ν_{Ti}(OH) and ν_V(OH) bands, the ν_P(OH) band increased in intensity with increasing amount of P_2O_5. Since most part of the hydroxyl groups bonded to titanium and vanadium are replaced with the P–OH groups at higher P_2O_5 loading, the catalyst surface might be well covered with phosphorus species. As an aqueous solution of H_3PO_4 was used for impregnation, $O(HO)_2{=}O^-$ ions might preferentially coordinate around the surface hydroxyl groups on titanium as well as those on vanadium. During the preparation, a reaction may proceed between phosphorus species and titanium on the surface. Consequently, the P–OH groups replace the Ti–OH and V–OH groups.

The band due to the surface sulphate species decreases in intensity with increasing amount of P_2O_5 addition, and almost disappears above 2 wt% P_2O_5 loading (not shown

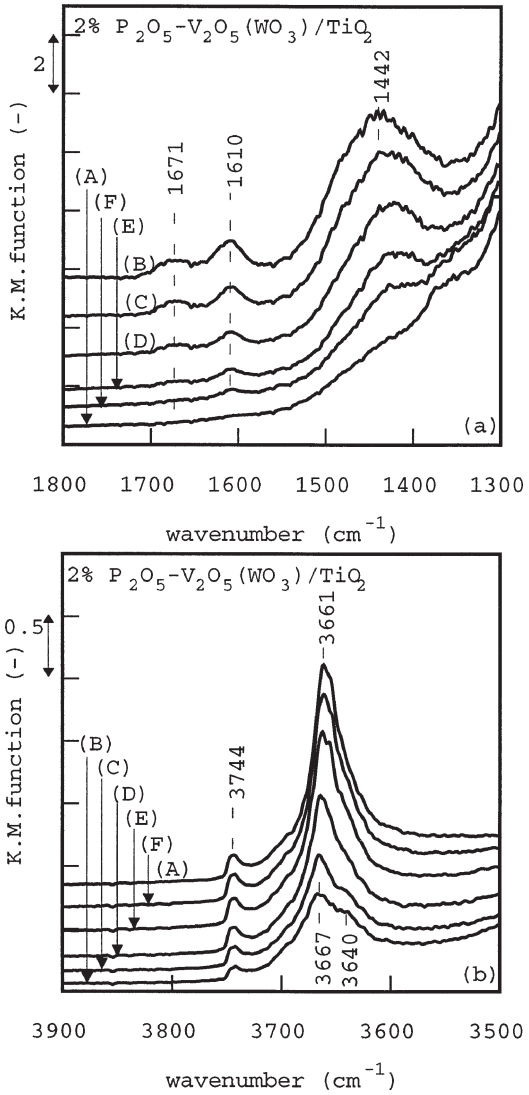

Figure 5. DRIFT spectra of NH_3 adsorption on $V_2O_5(WO_3)/TiO_2$ with 2 wt% P_2O_5 content. Two spectral regions, 1800–1300 and 3900–3500 cm^{-1}, are shown in (a) and (b), respectively. (A) After being heated at 593 K under flowing argon for 3 h, (B) after being exposed to gaseous NH_3 for 30 min and subsequently purged by argon for 30 min at room temperature, and (C)–(F) after being heated at 373 (C), 473 (D), 523 (E), and 573 K (F) under a stream of argon. All spectra were collected at room temperature.

in figure). The disappearance of sulphate species would contribute to the decrease of the acid strength.

After being exposed to gaseous NH_3, all samples with addition of phosphorus also show the characteristic feature of NH_3 adsorbed on them. Figure 5 shows DRIFT spectra of NH_3 adsorbed on the sample with 2 wt% P_2O_5 content as an example. When the catalyst is exposed to gaseous NH_3, the ν_P(OH) band decreases readily in intensity. With increasing activation temperature, both $\delta_{as}(NH_4^+)$ and $\delta_s(NH_3)$ bands decrease in intensity. Correspondingly, the intensity of the ν_P(OH) band is restored to its original intensity. This implies that the P–OH groups are also responsible for the Brønsted acidity. Compared with the V–OH groups, the acid strength of the P–OH groups may

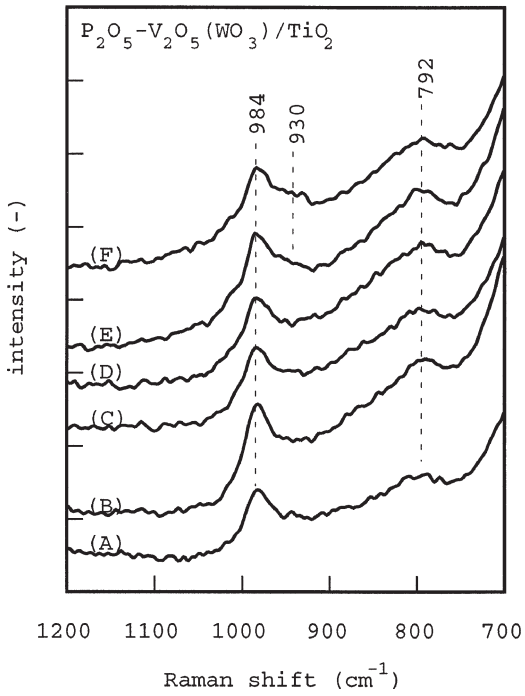

Figure 6. Raman spectra of $V_2O_5(WO_3)/TiO_2$ with different P_2O_5 contents under ambient conditions. (A) 0, (B) 0.1, (C) 1, (D) 2, (E) 3, and (F) 5 wt% P_2O_5.

be weaker, because the intensity of the ν_P(OH) band is readily restored to its original intensity at the lower temperatures of the heat treatment.

3.5. Surface vanadyl and wolframyl species

Figure 6 shows Raman spectra of the $V_2O_5(WO_3)/TiO_2$ catalyst with different P_2O_5 contents under ambient conditions collected at 50 mW of laser power. A strong Raman band is present at 984 cm^{-1} for all samples, which is characteristic of the terminal V=O group, $\nu_{V=O}$, of the hydrated surface vanadyl species [23]. Up to 5 wt% P_2O_5 loading, the position of the $\nu_{V=O}$ band does not change, suggesting that phosphorus does not significantly modify the structure of the surface V=O species. At higher amounts of P_2O_5 addition, a Raman band becomes visible at around 930 cm^{-1}, indicating an interaction between phosphorus and the surface species, with the possible formation of $VOPO_4$ [24]. The Raman band of the terminal W=O groups is not observed in this study because of the lower intensity of the W=O groups compared to that of V=O groups [23].

According to Deo and Wachs [9], the molecular structure of the surface vanadyl species is controlled by the net pH at point of zero charge (pzc) under hydrated conditions, because the catalyst surface is covered with water molecules. Christiani et al. [25] reported that the change in the Raman band of surface vanadyl species on increasing laser power for a 10 wt% V_2O_5/TiO_2 catalyst was due to the dehydration of the catalyst surface. Their observations showed that the band near 995 cm^{-1} decreases in intensity, while that at 1030 cm^{-1} increases with increasing laser power.

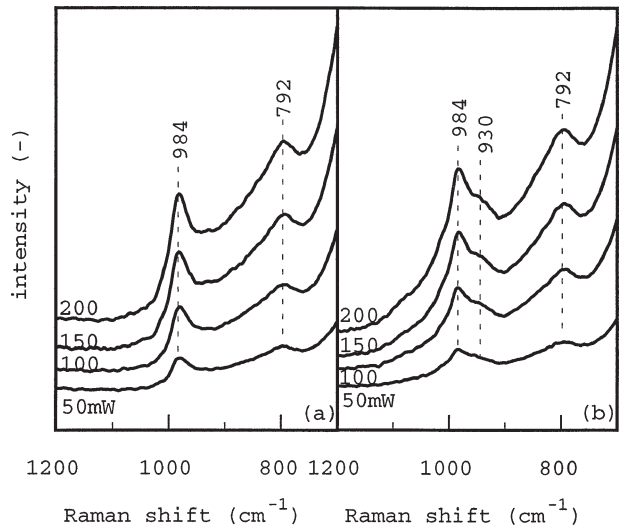

Figure 7. Raman spectra of $V_2O_5(WO_3)/TiO_2$ without P_2O_5 (a) and with 5 wt% P_2O_5 (b) on increasing laser power from 50 to 200 mW.

These bands correspond to the hydrated and dehydrated forms of the terminal V=O groups, respectively [25]. To test whether the molecular structure of the surface species changes upon dehydration, we also collected the Raman spectra on increasing laser power up to 200 mW, which would dehydrate the surface of the catalyst. As shown in figure 7, the position of the $\nu_{V=O}$ band does not change on increasing laser power, irrespective of the dehydration of the surface. The results obtained in this study imply that, on the commercial SCR catalyst, the surface vanadyl species are strongly immobilised on the surface of TiO_2 and, probably, also on WO_3. Consequently, the water molecules on the surface would not significantly affect them. The structure of the surface species, however, has not been clarified in detail. Since the Raman band broadens (compare figure 7 (a) and (b)), the phosphorus-containing species should cover the catalyst surface as expected by XPS and infrared spectroscopy.

At higher oxygen concentrations, for example, above 1%, the reaction rate does not significantly depend on the oxygen concentration [26,27]. Topsøe et al. [28] suggested that both Brønsted acid sites and the V=O groups are involved in the SCR reaction. The re-oxidation step of the surface V=O groups, however, might not be a rate-limiting step for the V_2O_5/TiO_2 catalyst under higher oxygen concentrations [28]. Since the phosphorus species might cover the majority of the surface at higher loadings, the terminal V=O and W=O groups may be partially covered by phosphorus species. The decrease in the NO reduction activity, due to the blockage of the surface V=O and W=O groups, therefore would become noticeable at lower oxygen concentrations. The hydroxyl groups bonded to phosphorus species, P–OH, still have a certain extent of Brønsted acidity, although their strength is weaker than that of the V–OH groups. Consequently, the P–OH groups could also assist to activate adsorbed NH_3 for the NO reduction without significant deactivation.

4. Conclusions

Large amounts of phosphorus modify the textural properties of the catalyst due to the interaction with the TiO_2 carrier as well as with V_2O_5 and WO_3. Phosphorus added to the catalyst replaces the surface hydroxyl groups with those bonded to phosphorus, P–OH. The P–OH groups still have a certain strength of Brønsted acidity, which can also activate adsorbed ammonia for the subsequent NO reduction. Large amounts of phosphorus as contamination eliminate the sulphur species on the catalyst surface, which would also result in a decrease of the acid strength. The deactivation of the catalyst might be caused by the alteration of the nature of the acid sites, probably the Brønsted acid sites. Phosphorus species might partially wrap the surface V=O and W=O groups, which may also contribute to the deactivation.

Acknowledgement

We are grateful to Mrs. Birgitta Svensson for technical assistance and to Mrs. Raziyeh Khodayari for helpful support. We gratefully acknowledge Dr. Arne Andersson for stimulating discussions. The financial support from Japan Cooperation Center Petroleum (JCCP) is also acknowledged.

References

[1] H. Bosch and F.J.J.G. Janssen, Catal. Today 2 (1988) 369.
[2] G.T. Went, L.-J. Leu and A.T. Bell, J. Catal. 134 (1992) 479.
[3] C. Cristiani, G. Busca and P. Forzatti, J. Catal. 116 (1989) 586.
[4] T. Shikada and K. Fujimoto, Chem. Lett. (1983) 77.
[5] S. Kasaoka, E. Sasaoka and H. Nanba, Nippon Kagaku Kaishi (1984) 486.
[6] L. Lietti, P. Forzatti, G. Ramis, G. Busca and F. Bregani, Appl. Catal. B 3 (1993) 13.
[7] H. Bosch, A. Bongers, G. Enoch, R. Snel and J.R.H. Ross, Catal. Today 4 (1989) 139.
[8] J.P. Chen and R.T. Yang, J. Catal. 125 (1990) 411.
[9] G. Deo and I.E. Wachs, J. Phys. Chem. 95 (1991) 5889.
[10] G. Deo and I.E. Wachs, J. Catal. 146 (1994) 335.
[11] J.P. Chen, M.A. Buzanowski, R.T. Yang and J.E. Cichanowicz, J. Air Waste Manag. Assoc. 40 (1990) 1403.
[12] J. Blanco, P. Avila, C. Barthelemy, A. Bahamonde, J.A. Odriozola, J.F. Garcia De La Banda and H. Heinemann, Appl. Catal. 55 (1989) 151.
[13] M. Ai, Bull. Chem. Soc. Jpn. 50 (1977) 355.
[14] J. Zhu, B. Rebenstorf and S.L.T. Andersson, J. Chem. Soc. Faraday Trans. I 85 (1989) 3645.
[15] G.C. Bond and S.F. Tahir, Catal. Today 10 (1991) 393.
[16] A.J. van Hengstum, J. Pranger, J.G. van Ommen and P.J. Gellings, Appl. Catal. 11 (1984) 317.
[17] C.U.I. Odenbrand, S.T. Lundin and L.A.H. Andersson, Appl. Catal. 18 (1985) 335.
[18] H. Kamata, K. Takahashi and C.U.I. Odenbrand, to be submitted.
[19] G. Busca, H. Saussey, O. Saur, J.C. Lavalley and V. Lorenzelli, Appl. Catal. 14 (1985) 245.
[20] G. Busca and L. Marchetti, J. Chem. Soc. Faraday Trans. I 81 (1985) 1003.
[21] G. Busca, Langmuir 2 (1986) 577.

[22] N.Y. Topsøe, J. Catal. 128 (1991) 499.
[23] M.A. Vuurman, I.E. Wachs and A.M. Hirt, J. Phys. Chem. 95 (1991) 9928.
[24] F.B. Abdelouahab, R. Olier, N. Guilhaume, F. Lefebvre and J.C. Volta, J. Catal. 134 (1992) 151.
[25] C. Cristiani, P. Forzatti and G. Busca, J. Catal. 116 (1989) 586.
[26] C.U.I. Odenbrand, S.T. Lundin and L.A.H. Andersson, Appl. Catal. 18 (1985) 335.
[27] C.U.I. Odenbrand, A. Bahamonde, P. Avila and J. Blanco, Appl. Catal. B 5 (1994) 117.
[28] N.-Y. Topsøe, H. Topsøe and J.A. Dumesic, J. Catal. 151 (1995) 241.